Chapter 5

The Witten-Veneziano formula

In this chapter we compute the decay constant of the η meson, F_η, in two dimensions and attempt to make a connection with the value of F_π that we measured in the previous chapter. To do so we rely on the Witten-Veneziano formula [1,2], which in 3-flavor QCD relates the mass of the η' meson with m_η, m_K, F_π and the quenched *topological susceptibility* $\chi_T^{\rm que}$, defined below. This formula is obtained by taking the *t'Hooft limit* of a $1/N_c$ expansion, where N_c is the color number. In this limit one considers $N_c \to \infty$ and $g_s \to 0$, but leaving the product $g^2 = g_s^2 N_c$ finite (g_s is the strong coupling constant).

In theory one introduces two eta mesons, with the valence quark composition

$$\eta_8 = \frac{1}{\sqrt{6}}\left(\overline{u}u + \overline{d}d - 2\overline{s}s\right), \quad \eta_1 = \frac{1}{\sqrt{3}}\left(\overline{u}u + \overline{d}d + \overline{s}s\right). \tag{5.1}$$

η_8 belongs to an octet of states, while η_1 to a singlet. In nature one observes the particles η and η', which are mixed by an angle θ_P

$$\begin{pmatrix}\eta \\ \eta'\end{pmatrix} = \begin{pmatrix}\cos\theta_P & -\sin\theta_P \\ \sin\theta_P & \cos\theta_P\end{pmatrix}\begin{pmatrix}\eta_8 \\ \eta_1\end{pmatrix}. \tag{5.2}$$

Since the measured value of θ_P is $-11.3°$ [3], we have

$$\eta \approx \frac{1}{\sqrt{6}}\left(\overline{u}u + \overline{d}d - 2\overline{s}s\right), \quad \eta' \approx \frac{1}{\sqrt{3}}\left(\overline{u}u + \overline{d}d + \overline{s}s\right). \tag{5.3}$$

Veneziano obtained the following formula by taking into account the three lightest quark flavors

$$m_{\eta'}^2 + m_\eta^2 - 2m_K^2 = \frac{6}{F_{\eta'}^2}\chi_T^{\rm que}. \tag{5.4}$$

where $F_{\eta'}$ is the decay constant of the meson η' and "que" stands for quenched, *i.e.* its value when the degenerate fermion mass $m \to \infty$. To lowest order in a $1/N_c$ expansion, we have $F_{\eta'} = F_\pi$ in QCD [1]. In the chiral limit we obtain the formula deduced by E. Witten

$$m_{\eta'} = \frac{6}{F_{\eta'}^2}\chi_T^{\rm que}. \tag{5.5}$$

In general, the literature refers to eq. (5.4) as the Witten-Veneizano formula.

In the two-flavor Schwinger model, in the limit of massless fermions, eq. (5.4) is simplified to[1] [4, 5]

$$m_\eta^2 = \frac{2N}{F_\eta^2}\chi_T^{\text{que}}, \tag{5.6}$$

where N is the number of flavors. Below eq. (38) of ref. [6], the authors seem to claim that $F_\eta = F_\pi$ is valid in QED$_2$ as well, but they are ambiguous about it. Still, we compute F_η in the Schwinger model with eq. (5.6) and based on the final result we verify whether the relation $F_\eta = F_\pi$ holds. This would also enable us to determine F_π by an independent method that does not involve the δ-regime.

The topological susceptibility χ_T is defined for the Euclidean Schwinger model in the continuum as

$$\chi_T = \int d^2x\, \left(\langle q(x)q(0)\rangle - \langle q(x)\rangle\langle q(0)\rangle\right), \tag{5.7}$$

where

$$q(x) = \frac{g}{4\pi}\epsilon_{\mu\nu}F_{\mu\nu}(x) = \frac{g}{2\pi}F_{12}(x) \tag{5.8}$$

is the *topological charge density.* With $q(x)$ we define the *topological charge* as

$$Q = \int d^2x\, q(x). \tag{5.9}$$

We can formulate χ_T in terms of Q as well

$$\chi_T = \frac{\langle Q^2\rangle - \langle Q\rangle^2}{V}, \tag{5.10}$$

where V is the space-time volume. An important property of the topological charge is that it is an integer number. We can see that fact if we rewrite $q(x)$ as a total divergence

$$q(x) = \partial_\mu\Omega_\mu(x), \quad \Omega_\mu(x) = \frac{g}{2\pi}\epsilon_{\mu\nu}A_\nu(x). \tag{5.11}$$

If we consider field configurations of finite action, $F_{\mu\nu}(x)$ has to vanish at infinity, so the gauge field must be gauge equivalent to 0 when $|x| \to \infty$

$$0 = A'_\mu(x) = A_\mu(x) - \frac{1}{g}\partial_\mu\varphi(x). \tag{5.12}$$

Then

$$Q = \int d^2x\, \partial_\mu\left(\frac{g}{2\pi}\epsilon_{\mu\nu}\frac{1}{g}\partial_\nu\varphi(x)\right) = \frac{1}{2\pi}\int_{\partial V} d\sigma_\mu\, \epsilon_{\mu\nu}\partial_\nu\varphi(x), \tag{5.13}$$

where we have used the Gauss theorem and where we assume ∂V to be the boundary of a large volume in $\mathbb{R}^2$. Now, if we consider a circumference of length L, we identify Q with the following integral

$$\lim_{L\to\infty}\frac{1}{2\pi i}\int_0^L dx\, U^*(x)\partial_x U(x), \quad \text{where} \quad U(x) = e^{i\varphi(x)}, \quad U(L) = U(0). \tag{5.14}$$

This expression is equal to

$$\frac{1}{2\pi}\left[\varphi(L) - \varphi(0)\right] = n \in \mathbb{Z}, \tag{5.15}$$

hence Q is an integer.

[1] According to the literature [4, 5], the most suitable analogy of the heaviest meson of the two-flavor Schwinger model, whose fermion composition is analogous to $(\overline{u}u + \overline{d}d)/\sqrt{2}$, with QCD would be η'; however, it is not the actual η' particle from QCD and for simplicity we will denote it as η.

As we mentioned in Chapter 3, we can relate m_η with the gauge coupling as follows

$$m_\eta^2 = N\frac{g^2}{\pi}. \tag{5.16}$$

Thus, by determining χ_T we obtain a value for F_η. According to refs. [4,5], the theoretical expression for χ_T^{que} in infinite volume and in the continuum is

$$\chi_T^{\text{que}} = \frac{g^2}{4\pi^2} \simeq 0.0253\, g^2. \tag{5.17}$$

On the other hand, to measure the topological susceptibility by using lattice simulations we have to discretize the topological charge density. This can be done through the plaquette variables defined in Chapter 2. From eq. (2.94), we know that for a small lattice spacing a, the plaquettes have the following expression

$$U_{\mu\nu}(\vec{n}) = e^{iga^2 F_{\mu\nu}(\vec{n})}, \quad F_{\mu\nu}(\vec{n}) = -\frac{i}{ga^2}\ln U_{\mu\nu}(\vec{n}). \tag{5.18}$$

That way, we have

$$q(\vec{n}) = -\frac{i}{2\pi a^2}\ln U_{12}(\vec{n}) \tag{5.19}$$

and

$$Q = \sum_{\vec{n}\in\mathbb{V}} a^2 q(\vec{n}), \tag{5.20}$$

where $\mathbb{V} = \{\vec{n} = (n_1, n_2)|\, n_\mu = 0, 1, \ldots, N_\mu - 1; \mu = 1, 2\}$ is the set of lattice sites.

The lattice configurations generated through Monte Carlo algorithms are sorted in different sectors, where each one is characterized by a topological charge. Furthermore, there is evidence (see e.g. refs. [7, 8]) that the distribution of these configurations corresponds approximately to a Gaussian function. Due to parity symmetry, we also have

$$\langle Q\rangle = 0. \tag{5.21}$$

Then, one can calculate χ_T on the lattice using the following weighted average

$$\chi_T = \frac{\sum_Q Q^2\, N_Q}{V\sum_Q N_Q}, \tag{5.22}$$

where N_Q are the number of configurations in the topological sector labeled by Q.

In Chapter 5 we have shown the histograms for Q obtained with simulations for several lattice sizes, using low statistics (10^3 measurements separated by 10 sweeps). We attempted to compute the topological susceptibility using those results. Unfortunately, even though the topological charge is compatible with $\langle Q\rangle = 0$, χ_T as a function of the fermion mass m does not have a clear behavior, see for instance figure 5.1. This does not allow us to perform a fit and to extrapolate to the quenched value of χ_T. For that reason, we incremented the number of measurements to 10^4, separated by 100 sweeps, and simulated a 10×64 lattice for $\beta = 4$. This improved the results. In figure 5.2 we show the distribution of the configurations and in figure 5.3 we show the topological susceptibility as a function of the degenerate fermion mass. We used two functions to extrapolate χ_T, from their average we obtain

$$\chi_T^{\text{que}}\beta = 0.029(1). \tag{5.23}$$

This result is in agreement with ref. [9], where they measured $\chi_T^{\text{que}}\beta = 0.0300(8)$ for $\beta = 4$.

Now, we substitute eq. (5.16) in eq. (5.6) and solve for F_η

$$F_\eta^2 = \chi_T^{\text{que}} \frac{2\pi}{g^2}. \tag{5.24}$$

Using the result in eq. (5.23) yields

$$F_\eta = 0.4243(76). \tag{5.25}$$

To check the lattice artifacts of this quantity, we compute F_η for more values of β.

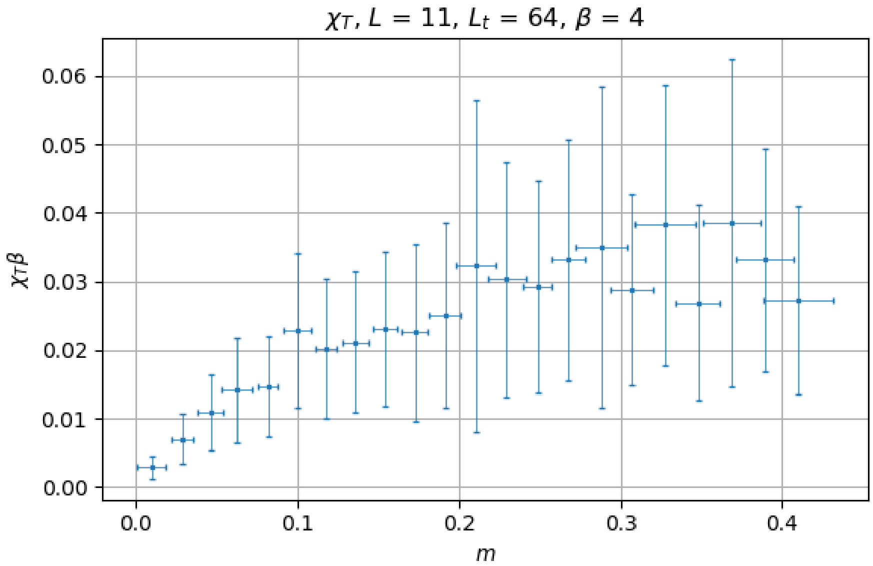

Figure 5.1: Topological susceptibility as a function of the fermion mass m, computed for 10^3 measurements with 10 sweeps between each of them on a 11×64 lattice. χ_T does not have a clear behavior for this number of measurements.

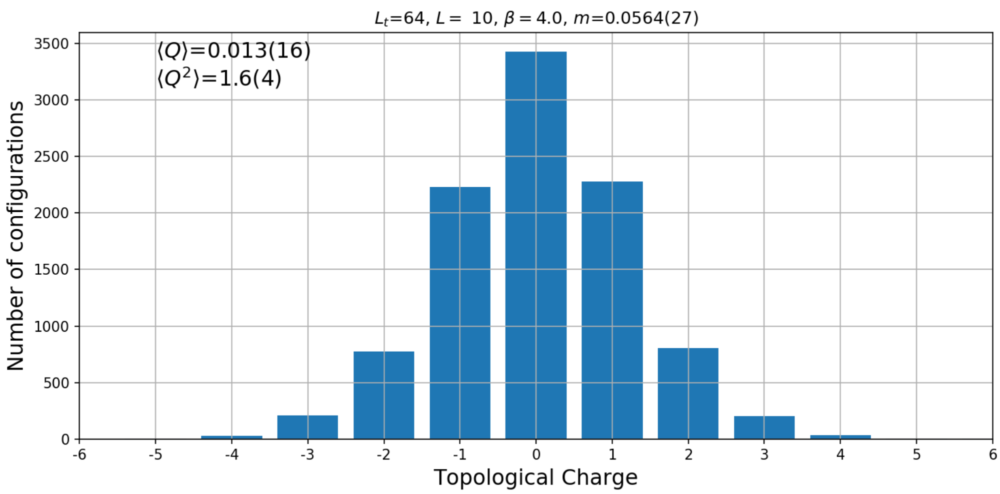

(a) Configurations sorted by their topological charge for $m = 0.0564(27)$.

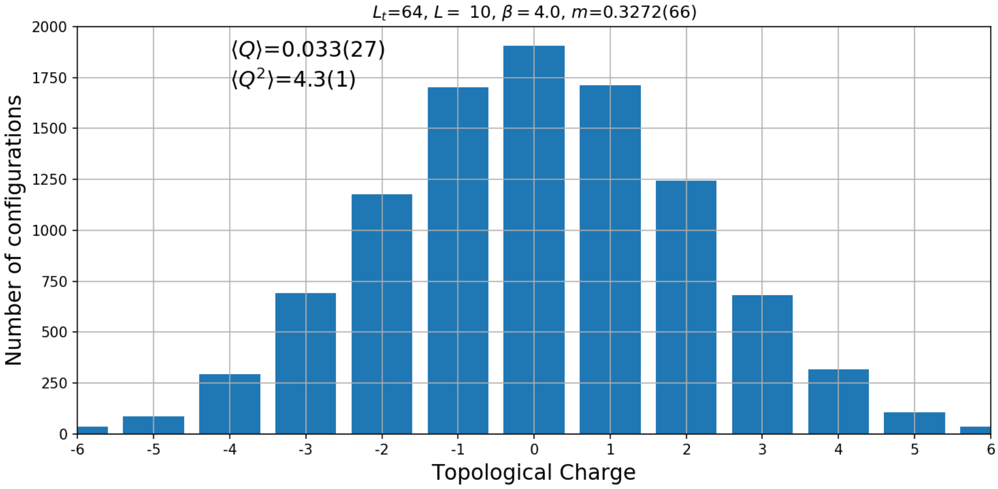

(b) Configurations sorted by their topological charge for $m = 0.3272(66)$.

Figure 5.2: Distribution of the Monte Carlo configurations in different topological sectors for $\beta = 4$. We see approximately a Gaussian distribution. m denotes the degenerate PCAC fermion mass. When the mass is smaller, the configurations occupy less topological sectors.

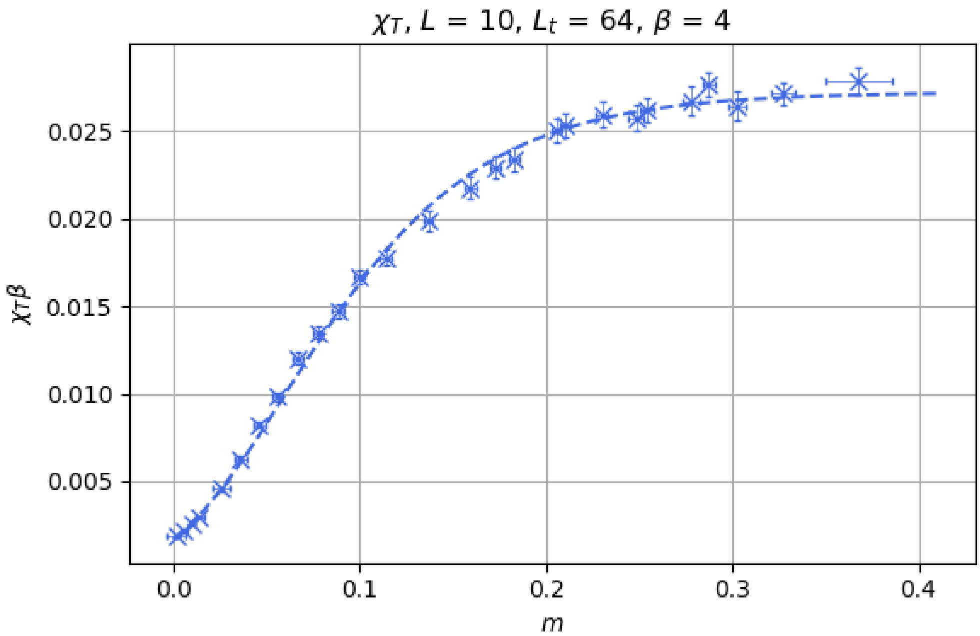

(a) A function of the form $y = ae^{-be^{-cx}}$ was fitted to the data.

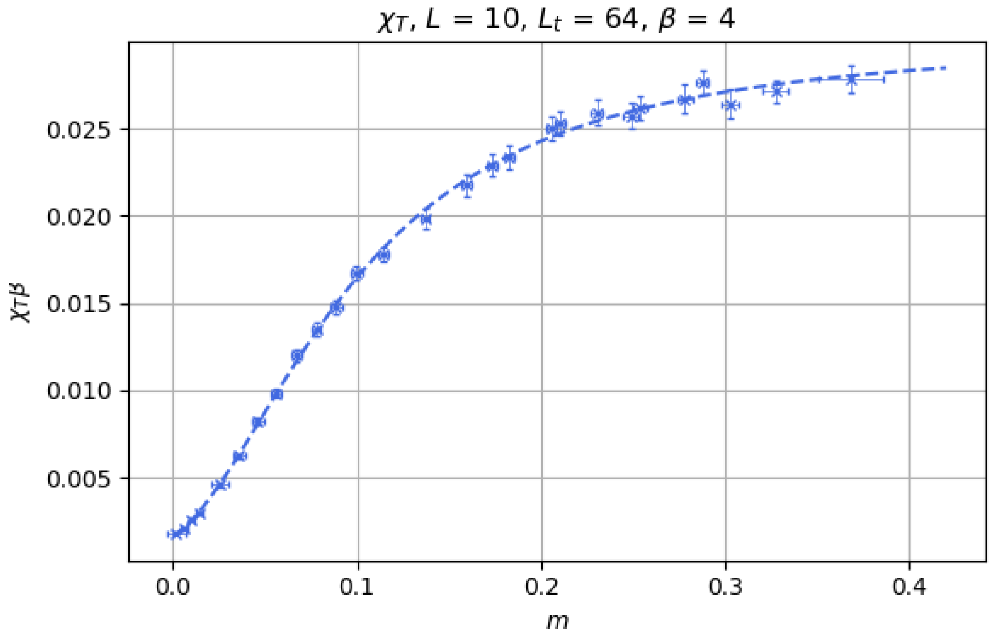

(b) We also fitted a function of the form $y = \frac{a+bx+cx^2}{d+fx+gx^2}$.

Figure 5.3: Topological susceptibility as a function of the degenerate fermion mass obtained with 10^4 measurements. The plots are in lattice unites. We performed two fits in order to extract the value of χ_T when $m \to \infty$. The results yield $\chi_T^{\text{que}}/g^2 = \chi_T^{\text{que}}\beta = 0.029(1)$.

To do so, we performed more simulations to determine χ_T in the quenched approximation by working with pure gauge theory, *i.e.* by generating Monte Carlo configurations using only the gauge action

$$S_G = \frac{1}{4}\int d^4x\, F_{\mu\nu}F_{\mu\nu}. \tag{5.26}$$

This is more convenient than extrapolating χ_T to infinite m, because the simulations are faster and they yield results for $m \to \infty$. Still, the extrapolation of χ_T to infinite m works as a cross-check with the results of $\beta = 4$ that we obtain with the quenched simulations.

In figure 5.4, we show $\chi_T^{\text{que}}\beta$ for different lattices of dimension $L \times L$ and $\beta = 2, 3, 4, 5, 6, 7$ and 8. We took 10^4 measurements separated by 10 sweeps for $\beta = 2, 3$; 10^4 measurements separated by 100 sweeps for $\beta = 4$ and 5 and 10^4 measurements separated by 10^3 sweeps for $\beta = 6, 7$ and 8 . In table 5.1 we show $\chi_T^{\text{que}}\beta$ for the different β values that we simulated, together with F_η computed with the Witten-Veneziano formula.

β	$\chi_T^{\text{que}}\beta$	F_η
2	0.0389(2)	0.495(1)
3	0.0335(3)	0.459(2)
4	0.0304(2)	0.437(1)
5	0.0285(4)	0.423(3)
6	0.0283(4)	0.422(2)
7	0.0261(11)	0.404(9)
8	0.0256(19)	0.399(15)

Table 5.1: Results of $\chi_T^{\text{que}}\beta$ and F_η for different β values obtained with pure gauge theory simulations.

We observe that χ_T^{que} strongly depends on β. As β increases, $\chi_T^{\text{que}}\beta$ decreases monotonically. For $\beta = 4$ the number that we obtain by means of the quenched simulations is compatible, within errors, with the large m extrapolation that we performed before. In figure 5.5, we show a comparison of our results for $\chi_T^{\text{que}}\beta$ with the values of refs. [5,9]. We see that the lattice results are above the theoretical prediction, given by eq. (5.17), and they seem to converge to it for large β, which is the continuum limit. Since $\chi_T^{\text{que}}\beta$ is not independent of β, F_η also has lattice artifacts. We can perform an extrapolation to the continuum limit by fitting the ansatz $\chi_T^{\text{que}}\beta = a + b/\beta$, where a and b are fit parameters, in order to determine F_η. The extrapolation yields

$$\chi_T^{\text{que}}\beta = 0.0223(3), \quad F_\eta = 0.374(3). \tag{5.27}$$

The result of eq. (5.27) is slightly below the theoretical prediction for infinite volume and in the continuum, given by eq. (5.17). We also compare our result of $\chi_T^{\text{que}}\beta$ for large β with the value that was obtained in ref. [10]: $\chi_T^{\text{que}}\beta \simeq 0.023$. Our result is in agreement with this value.

Also, when we compare F_η with the value that we obtained in the δ-regime: $F_\pi = 0.6688(5)$, we observe that they do not agree. Furthermore, in the δ-regime the result was independent of β and the lattice artifacts were mild, in contrast to the outcome of F_η. This confirms that the hypothesis that F_η could be equal to F_π in the Schwinger model is not correct, although they are of the same order of magnitude. Even so, the method presented in this chapter could be useful in the context of QCD to determine F_π with lattice simulations.

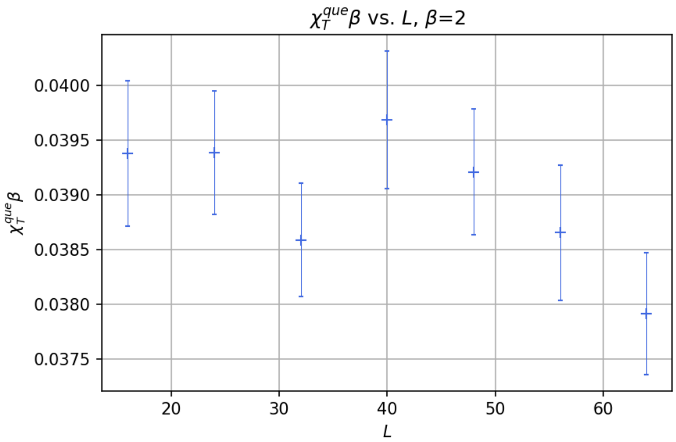

(a) $\chi_T^{\text{que}}\beta$ vs. L for $\beta = 2$. An average yields $\chi_T^{\text{que}} = 0.0389(2)$.

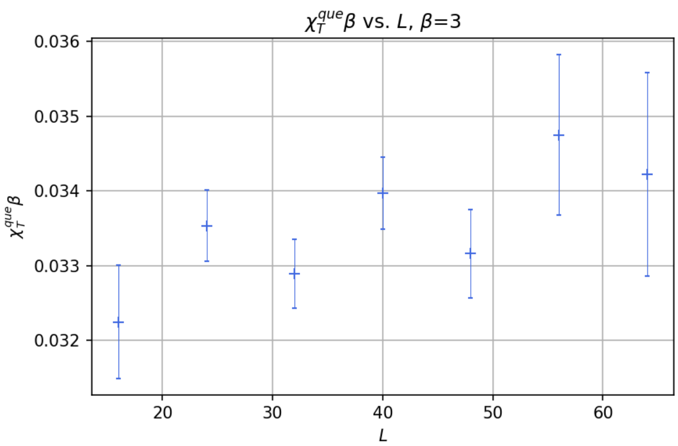

(b) $\chi_T^{\text{que}}\beta$ vs. L for $\beta = 3$. An average yields $\chi_T^{\text{que}} = 0.0335(3)$.

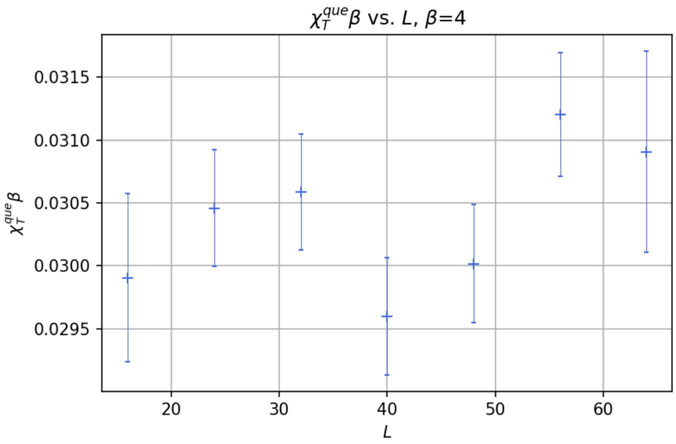

(c) $\chi_T^{\text{que}}\beta$ vs. L for $\beta = 4$. An average yields $\chi_T^{\text{que}} = 0.0304(2)$.

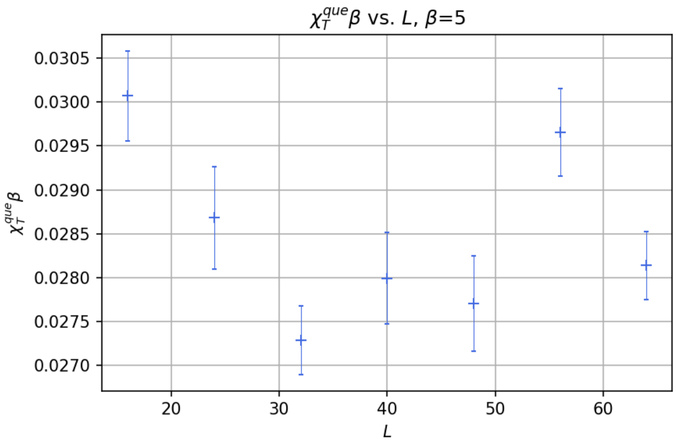

(d) $\chi_T^{\text{que}}\beta$ vs. L for $\beta = 5$. An average yields $\chi_T^{\text{que}} = 0.0285(4)$.

Figure 5.4: $\chi_T\beta$ measured for different β and lattices of dimensions $L \times L$

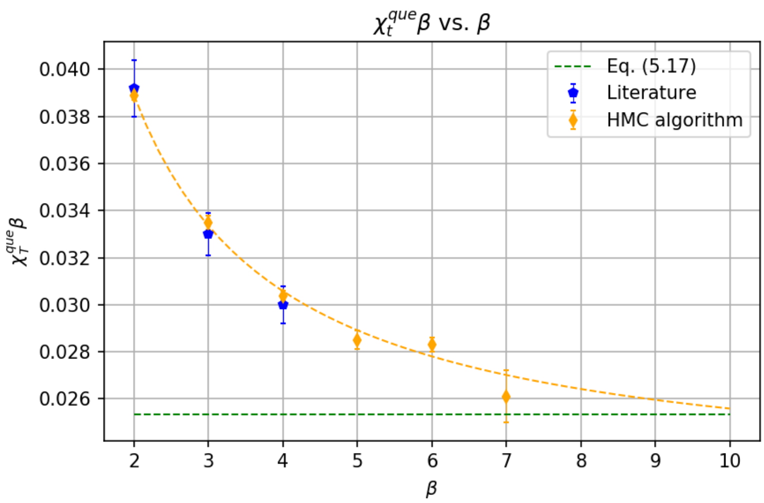

Figure 5.5: $\chi_T^{\text{que}}\beta$ vs. β. The literature values correspond to ref. [9]. HMC algorithm denotes the results that we computed with pure gauge theory simulations. In order to determine $\chi_T^{\text{que}}\beta$ in the continuum we fitted a function of the form $y = a + b/x$, which yielded $\chi_T^{\text{que}}\beta = 0.0223(3)$.

Bibliography

[1] E. Witten. Current Algebra Theorems for the U(1) Goldstone Boson. *Nucl. Phys. B*, 156:269–283, 1979.

[2] G. Veneziano. U(1) Without Instantons. *Nucl. Phys. B*, 159:213–224, 1979.

[3] P.A. Zyla et al. Review of Particle Physics. *Prog. Theor. Exp. Phys.*, 2020:083C01, 2020.

[4] E. Seiler and I. O. Stamatescu. Some remarks on the Witten-Veneziano formula for the η' mass. *MPI-PAE-PTh-10-87*.

[5] E. Seiler. Some more remarks on the Witten-Veneziano formula for the eta-prime mass. *Phys. Lett. B*, 525:355–359, 2002.

[6] C. Gattringer and E. Seiler. Functional integral approach to the N flavor Schwinger model. *Ann. Phys.*, 233:97–124, 1994.

[7] C. R. Gattringer, I. Hip, and C. B. Lang. Quantum fluctuations versus topology: A Study in U(1)-2 lattice gauge theory. *Phys. Lett. B*, 409:371–376, 1997.

[8] S. Dürr, Z. Fodor, C. Hoelbling, and T. Kurth. Precision study of the SU(3) topological susceptibility in the continuum. *JHEP*, 04:055, 2007.

[9] I. Bautista, W. Bietenholz, A. Dromard, U. Gerber, L. Gonglach, C. P. Hofmann, H. Mejía, and M. Wagner. Measuring the Topological Susceptibility in a Fixed Sector. *Phys. Rev. D*, 92:114510, 2015.

[10] S. Dürr and C. Hoelbling. Scaling tests with dynamical overlap and rooted staggered fermions. *Phys. Rev. D*, 71:054501, 2005.